

# Spectroscopic elucidation of the interaction of native cyclodextrins and their acetylated derivatives with asymmetric monomethyne cyanine dye

E. Kostadinova · S. Kaloyanova · St. Stoyanov ·  
I. Petkov

Received: 5 July 2010 / Accepted: 19 February 2011 / Published online: 15 March 2011  
© Springer Science+Business Media B.V. 2011

**Abstract** Five novel complexes of asymmetric monomethyne cyanine dye (**1**), with  $\alpha$ -,  $\beta$ -,  $\gamma$ -cyclodextrins and the corresponding functionalized derivatives, namely acetyl- $\beta$ -(Ac- $\beta$ -CD) and acetyl- $\gamma$ -(Ac- $\gamma$ -CD) cyclodextrins were studied by means of UV–VIS, linear-polarized infrared and fluorescence spectroscopy, as well as scanning electron microscopy, powder X-ray diffraction, and thermal methods both in solution and in solid-state. Computational chemistry methods were employed with the purpose of elucidating the electronic structure and vibrational properties of the organic dye.

**Keywords** Asymmetric monomethyne cyanine dye · Native cyclodextrins · Acetylated-cyclodextrins · Supramolecular polymers

## Introduction

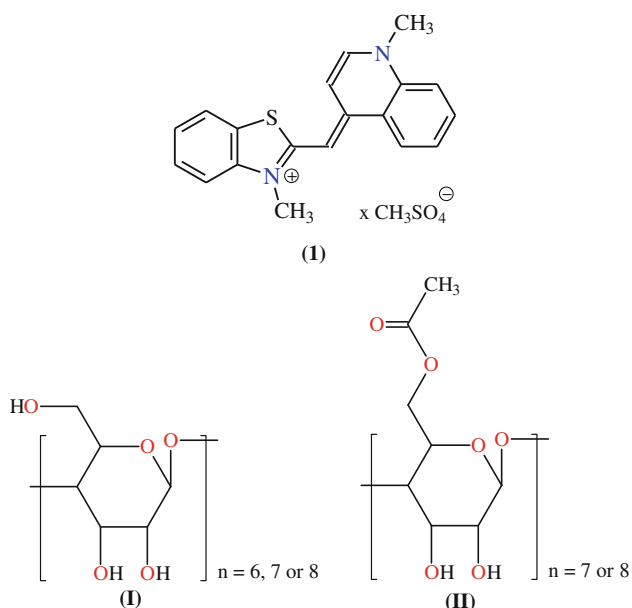
Native cyclodextrins (CDs) are among the most interesting and functional host natural materials [1–4], having a rigid, well-defined ring structure, with the shape of a truncated cone, and an ability to bind in their hydrophobic cavity various organic [3] and inorganic [4] molecules via hydrophobic, van der Waals, electrostatic and hydrogen bond interactions. Inclusion complexes of 1:1 and/or 1:2 stoichiometry (guest/host) have been widely observed in aqueous solutions [1–4] as a result of the combined action of several factors, as for example hydrophobicity, chirality, and most importantly the size/shape of the guest and the

size of the cyclodextrin macro ring employed. Moreover, it has been found that the interaction of appropriate linear oligomeric or polymeric chains with some CDs can lead to supramolecular assemblies such as rotaxanes [5, 6], polyrotaxanes [6–9], and threaded CDs [10], which do not involve any covalent bonding between the starting reactants. Another strategy for devising supramolecular architectures utilizes the interaction of CDs with some small rodlike molecules. Although the CDs themselves do not interact with each other in aqueous solutions, in the presence of an appropriate rodlike guest, the initially formed supramolecular building blocks, namely, singly occupied complexes are self-assembled to form complex architectures [11]. These architectures can be viewed as poly-pseudorotaxanes often referred to as “supramolecular polymers” [11].

The application of the organic dyes as guest molecules in host–guest systems with CDs has been used as strategy in crystal engineering for obtaining photodimeric products [12], with potential application in optical technologies.

Therefore herein we are presenting, the interaction of the asymmetric monomethyne cyanine dye (**1**), with native  $\alpha$ -,  $\beta$ -,  $\gamma$ -CDs and the corresponding functionalized derivatives acetyl- $\beta$ -(Ac- $\beta$ -CD) and acetyl- $\gamma$ -(Ac- $\gamma$ -CD) CDs (Scheme 1). The methods such as UV–VIS, fluorescence spectroscopy, linear-polarized infrared (IR-LD) spectroscopy of oriented colloids in nematic host,  $^1\text{H}$ -NMR spectroscopy, scanning electron microscopy (SEM), powder X-ray diffraction (XRD) as well as thermal methods were used. Theoretical quantum chemical calculations were also carried out with the purpose of obtaining the electronic spectra and vibrational properties of the isolated dye in order further to support the experimental elucidation of the optical properties of the inclusion complexes examined.

E. Kostadinova · S. Kaloyanova · St. Stoyanov · I. Petkov (✉)  
Faculty of Chemistry, Sofia University St. Kl. Ohridski,  
1, J. Bourchier Blvd, 1164 Sofia, Bulgaria  
e-mail: IPetkov@chem.uni-sofia.bg



**Scheme 1** Chemical formulas of the asymmetric monomethyne cyanine dye,  $\alpha$ - ( $n = 6$ ),  $\beta$ - ( $n = 7$ ) and  $\gamma$ - ( $n = 8$ ) cyclodextrins (I) and the functionalized derivatives, acetyl- $\beta$ - ( $n = 7$ ) and acetyl- $\gamma$ - ( $n = 8$ ) cyclodextrins (II)

## Experimental

### Materials and methods

*Conventional and polarized IR-spectra* were measured on a Thermo Nicolet FTIR-spectrometer ( $4000\text{--}400\text{ cm}^{-1}$ ,  $2\text{ cm}^{-1}$  resolution, 200 scans) equipped with a Specac wire-grid polarizer. Non-polarized solid-state IR-spectra were recorded using the KBr disk technique. The oriented samples were obtained as a colloid suspension in a nematic liquid crystal ZLI 1695. The theoretical approach, as well as the experimental technique for preparing the samples and the procedures for polarized IR-spectra interpretation, have been presented elsewhere [13–17]. The influence of the liquid crystal medium on peak positions and integral absorbances of the guest molecule bands, the rheological model, the nature and the balance of the forces in the nematic liquid crystal suspension system, as well as the morphology of the suspended particles have also been discussed [13].

$^1\text{H-NMR}$  measurements, referenced to sodium 3-(trimethylsilyl)-tetradeuteriopropionate, were made at 298 K with a Bruker DRX-400 spectrometer using 5 mm tubes and  $\text{D}_2\text{O}$  as solvent.

*Electronic (UV-Vis) spectra* were recorded on a Tecan Safire Absorbance/Fluorescence XFluor 4 V 4.40 and Evolution 300 spectrophotometers, operating between 190 and 900 nm, both in the solid-state and in solution at a concentration of  $2.5 \times 10^{-5}\text{ M}$ , using 0.0921 cm quartz cells.

The *thermal analyses* were performed in the range of 300–500 K on a Differential Scanning Calorimeter Perkin-Elmer DSC-7, and a Differential Thermal Analyzer DTA/TG (Seiko Instrument, model TG/DTA 300). The experiments were carried out at a scanning rate of 10 K/min under an argon atmosphere.

The *elemental analysis* was carried out according to the standard procedures for C and H (as  $\text{CO}_2$ , and  $\text{H}_2\text{O}$ ) and N (by the Dumas method).

*Scanning electron microscopy experiments* were performed on A HITACHI S-3500 N instrument.

The *photographs* of the plates were obtained on the Leica Microscope S3 with the LAS ES 1.6.0 software.

*X-ray powder diffraction patterns* were obtained using a Rigaku MiniFlex powder diffraction system, equipped with a horizontal goniometer in the  $\theta/2\text{--}\theta$  mode (Tokyo, Japan). The X-ray source was nickel-filtered  $\text{K}\alpha$  emission of copper ( $1.54056\text{ \AA}$ ). Samples were packed into an aluminum holder using a back-fill procedure and were scanned over the range of  $50\text{--}6^\circ 2\text{-}\theta$ , at a scan rate of  $0.5^\circ 2\text{-}\theta\text{ min}^{-1}$ . Using a data acquisition rate of one point per second, the scanning parameters equate to a step size of  $0.0084^\circ 2\text{-}\theta$ . Calibration of each powder pattern was effected using the characteristic scattering peaks of aluminum at  $44.738$  and  $38.472^\circ 2\text{-}\theta$ .

### Theoretical calculations

*Quantum chemical calculations* were performed with the GAUSSIAN 98 and Dalton 2.0 program packages [18, 19]. The output files are visualized by means of the ChemCraft program [20]. The geometries were optimized at the second-order Moller-Pleset perturbation theory (MP2) level, using the 6-31++G\*\* basis set. The molecular geometries of the studied species were fully optimized by the force gradient method using Bernys' algorithm. For each structure, the stationary points found on the molecule potential energy hyper surfaces were characterized using standard analytical harmonic vibrational analysis. The absence of imaginary frequencies (i.e., negative eigenvalues of the second-derivative matrix) confirmed that the stationary points correspond to minima on the potential energy hyper surfaces. The calculated vibrational frequencies and infrared intensities were checked to establish which kind of performed calculations agreed best with the experimental data. The MP2/6-31++G\*\* data are presented in the result and discussion part of the manuscript, where a modification of the results using the empirical scaling factor 0.8929 is made to achieve better correspondence between the experimental and the theoretical values. The UV spectra of the compound in the gas phase and in aqueous solution are obtained by CIS/6-311++G\*\* and TDDFT calculations.

## Synthesis

The dye 1-methyl-4-[(3-methyl-2(3*H*)-benzothiazolylidene)methyl]quinolinium methosulphate (**1**), was synthesized following the common scheme for the asymmetric monomethyne cyanine dyes [21]. A mixture of 0.01 mol of quaternary heterocyclic compound (Scheme 2, A) and 0.012 mol of sulfobetainic compound (Scheme 2, B) was suspended in 20 mL methoxyethanol and refluxed for 10 min. The reaction mixture was cooled and diethyl ether was added to the dye solution. The dye was precipitated as oil and the ether solution was decanted. The oil was dissolved in 50 mL ethanol, the solution was filtered hot, evaporated to 1–15 mL and after cooling the dye (**1**) was collected by filtration. After leaving to stand, red crystals were obtained from the resulting red solution and were filtered off and dried under air. (Found: C, 56.70; H, 4.84; N, 6.74; [C<sub>20</sub>H<sub>20</sub>N<sub>2</sub>S<sub>2</sub>O<sub>4</sub>] calcd.: C, 57.67; H, 4.84; N, 6.73%). The HPLC ESI MS–MS data show a formation of one reaction product. The TGV and DSC data in the temperature range of 300–500 K show an absence of the included solvent molecules.

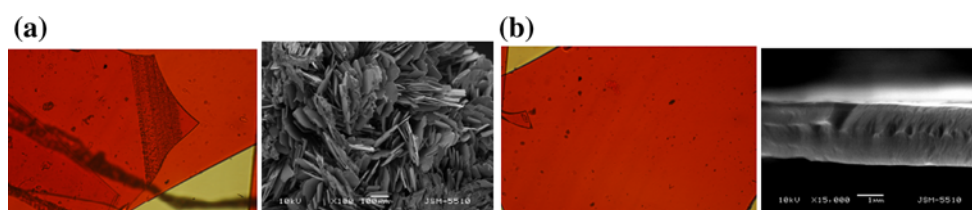
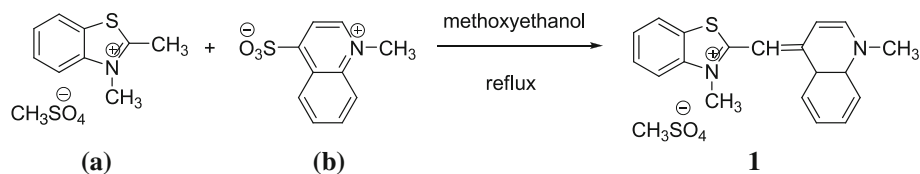
The “supramolecular polymers” of the CDs in the presence of (**1**) were obtained after mixing of equimolar amounts of each of the components in 20 mL aqueous solutions under continuous stirring and heating at 40 °C for 20 min. The obtained five new red–orange plates (Scheme 3) rest at

normal conditions for 7 weeks. The products were filtered off and dried on air at room temperature. <sup>1</sup>H-NMR measurements for all of the systems studied represent a superposition of the corresponding proton signals of the CDs and those of the dye (**1**). In the cases of the corresponding systems with the acetylated derivatives additionally are observed signals at 5.11 ppm of the OCH<sub>3</sub> groups. The proton signals of the dye could be assigned in a following way:  $\delta = 1.33$  ppm (s, 6H, N–CH<sub>3</sub>), AA'BB' signals  $\delta_{AA'}$ , 6.33, 6.41, 2H,  $\delta_{BB'}$ , 6.81, 6.90 ppm 2H, AB-signals 1H, 7.11, <sup>3</sup>J<sub>AB</sub> = 13.0 Hz, AA'BB' signals  $\delta_{AA'}$ , 7.48, 1H,  $\delta_{BB'}$ , 8.00, 8.07 ppm, 2H, 8.44, 8.46, 9.01 ppm, 3H, respectively.

## Results and discussion

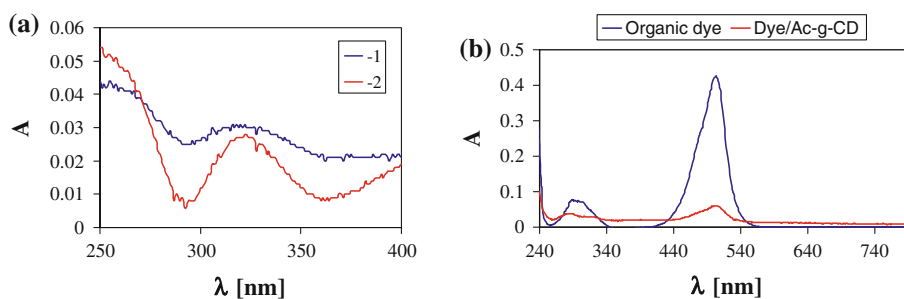
The electronic spectra of the starting  $\alpha$ -,  $\beta$ - and  $\gamma$ -CD display “transparency” in the whole range between 200 and 800 nm. The corresponding functionalized analogues of the CDs (**II**) (Scheme 1) are characterized with an absorption band around 325 nm with  $\epsilon_v$  within 89–102 L mol<sup>-1</sup> cm<sup>-1</sup> (Fig. 1a), which belongs to  $n \rightarrow \pi$  transition of the acetyl-substituent in the CDs. The UV–Vis spectrum of the organic dye (**1**) and the systems Dye/CDs are characterized with absorption bands about 290 ( $\epsilon_v \sim 1000$  L mol<sup>-1</sup> cm<sup>-1</sup>), 305 ( $\epsilon_v \sim 900$  L mol<sup>-1</sup> cm<sup>-1</sup>), 472 and 504 nm ( $\epsilon_v \sim 7000$  L mol<sup>-1</sup> cm<sup>-1</sup>), respectively. The first two maxima correspond to the B-band

**Scheme 2** Reaction scheme for synthesis of (**1**)



**Scheme 3** Photographs and SEM images of the systems (**1**)/Ac- $\beta$ -CD (**a**) and (**1**)/Ac- $\gamma$ -CD (**b**), respectively

**Fig. 1** UV–Vis spectra of **a** Ac- $\beta$ -CD (**1**) and Ac- $\gamma$ -CD (**2**) as well as **b** Dye (**1**) and the system Dye/Ac- $\gamma$ -CD in aqueous solution at  $2.5 \times 10^{-5}$  mol L<sup>-1</sup> concentration and 1 cm quartz cell



of the aromatic fragments, while the second ones in the visible region—to CT band in the dye (Fig. 1b). The keeping of the band position and profile is typical for the other CD–dye systems, where the corresponding organic dye is adsorbed on the CDs surfaces by weak van der Waals interactions. The most popular method for estimating the stoichiometry, the equilibrium constant and the molar absorptivity of non-covalent complexes is the Benesi-Hildebrand method [22]. In our previous paper, we have reported studies on some 2-styrylindolium dyes in aqueous solution and in the presence of CDs [23]. On the basis of the significant changes in the absorption behaviour of the supramolecular complexes, the Benesi-Hildebrand analysis has proven the suggested 1:1 stoichiometry. In contrast, the recorded absorption and fluorescence spectra of our present samples show no significant changes in presence of different concentrations of CDs. Therefore, we assume that supramolecular adsorption type complex is formed rather than classical inclusion one and the Benesi-Hildebrand method is not applicable for this particular case.

The data are in good correlation also with the theoretical electronic spectrum of the dye in aqueous solution, obtained by means of calculations at TD-DFT level of theory, giving bands at 290 ( $f = 0.0321$ ), 300 ( $f = 0.0451$ ), 465 ( $f = 0.1231$ ) and 500 ( $f = 0.2356$ ) nm, respectively. The HOMO and LUMO (Scheme 4) MOs gaps illustrate the CT transition in the dye, responsible for the observation of the absorption band in the visible region of the spectrum.

The observation of the interaction between the CDs and the dye molecule by means of the IR-spectroscopy is complicated and difficult task due to the strong overlap of the IR-bands of the CDs in the whole middle 4000–400  $\text{cm}^{-1}$  IR-region. Most of the previous studies [14, 17, 24–27] were found to deal with the vibration band assignments (both IR- and Raman) of the  $\nu_{\text{OH}}$  stretching vibrations within 3600–3000  $\text{cm}^{-1}$  (maximum about 3390  $\text{cm}^{-1}$  in Fig. 2). These regions are further complicated however by the fact that usually the CDs contain large number of solvent water molecules, displaying broad and intense absorption bands about 3300  $\text{cm}^{-1}$ , which additionally complicate the interpretation of the IR-spectroscopic patterns. The polarized IR-LD spectroscopy of oriented colloids in nematic host surmounts most of these difficulties, giving a possibility for experimental IR-band assignment as

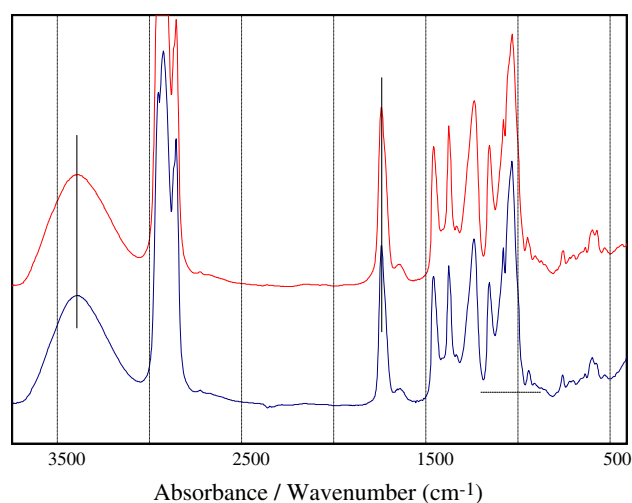
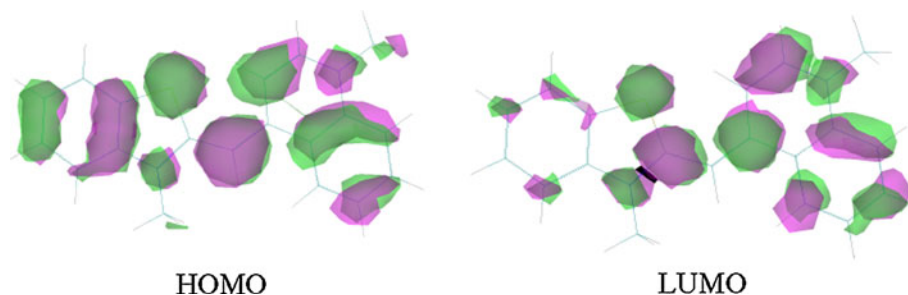


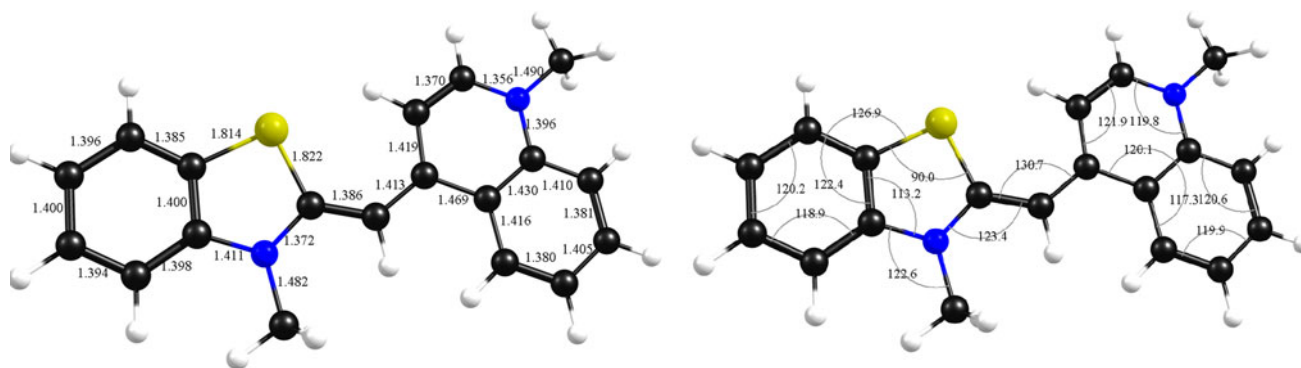
**Fig. 2** Solid-state IR-spectra of Ac- $\beta$ -CD (blue line) and Ac- $\gamma$ -CD (red line), respectively. (Color figure online)

well as “local structural” information for the guest–host systems. In the cases of the functionalized CDs additionally are observed the typical for the acetyl-group characteristic IR-bands of  $\nu_{\text{C=O}}$  stretching vibration about 1740  $\text{cm}^{-1}$  and within 1100–1000  $\text{cm}^{-1}$  (Fig. 2).

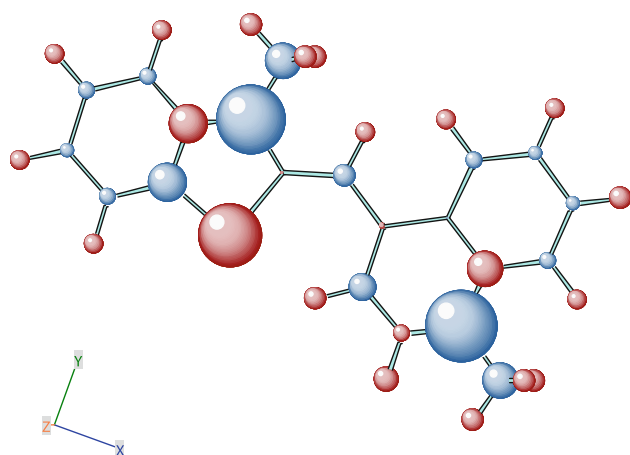
The capabilities of the polarized IR-LD spectroscopy were used for the assignment of the experimental IR-bands of the dye as well as those in the complexes with CDs. These data were compared with the corresponding theoretical estimates. The obtained vibrations are for the most stable conformer of the compound studied (Scheme 5). The geometry of the dye is effectively flat with 0.1° deviation from the perfect planarity. The N–CH<sub>3</sub> groups lies in the plane of the molecular skeleton with interplanar angles of 0.1(1)° and 0.00(3)°, respectively. For the purpose of the vibrational analysis, these data suggest that the transition moments of  $a''$  symmetry class of the aromatic fragments should be co-linear in principle with those of the out-of-plane  $\gamma_{\text{CH}}$  vibrations of the differently substituted double bonds (Scheme 1). However the theoretical calculations show a partial charge redistribution in the frame of the skeleton (Scheme 5), which affect as well on the obtained data of the bond lengths with the values within 1.372–1.420 Å (Scheme 6). The most intense bands in the

**Scheme 4** HOMO and LUMO MOs gaps of the dye





**Scheme 5** Most stable conformer and geometry parameters (bond lengths in Å, and angles in [°]) of the dye, optimized at MP2/6-31++G\*\* level of approximation



**Scheme 6** Single atomic charge redistribution

(**1**) are those of 1575, 1585, 1442, 1245 and 1213  $\text{cm}^{-1}$  which belong to the in-plane  $a'$  symmetry class (in terms of  $C_s$  symmetry of the molecule of (**1**)) as well as at 883 and 807  $\text{cm}^{-1}$  corresponding to  $a''$  out-of-plane vibrations (Fig. 3). The computed vibrations correlated well with the experimental values—a difference within 2–5  $\text{cm}^{-1}$ .

The experimental IR-LD spectroscopic analysis proves the suggested assignment of the characteristic IR-bands in the case of the pure dye as far as the subsequent elimination of the  $a'$  and  $a''$  bands is observed. In all cases the elimination of the given IR-band leads to observation of the second component, as a result of the presence of more than one non equivalent molecules in the unit cell [28–34], phenomenon typical for stilbazolium salts as well [35–38]. The IR-spectra of the CDs in the presence of (**1**), depicted in Fig. 4 are characterized with the overlapping effect of the characteristic IR-bands of the CDs and the (**1**). The intense bands about 3412  $\text{cm}^{-1}$  belong to the  $\nu_{\text{OH}}$  stretching vibrations of the OH groups in the CDs as well as of the clatrate solvent water molecules included in the CDs “supramolecular polymers”. The observation of the same

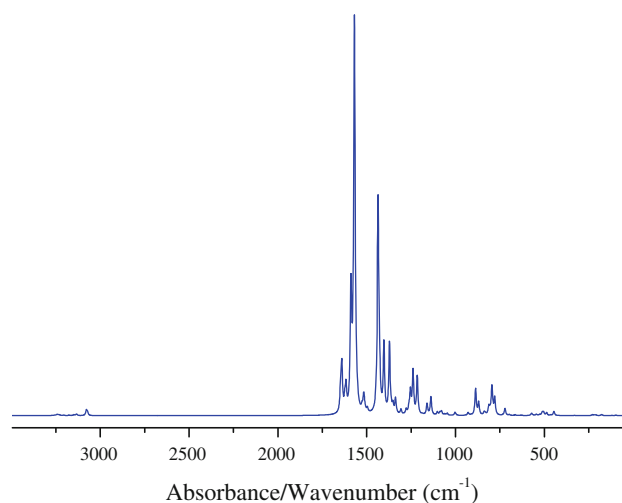


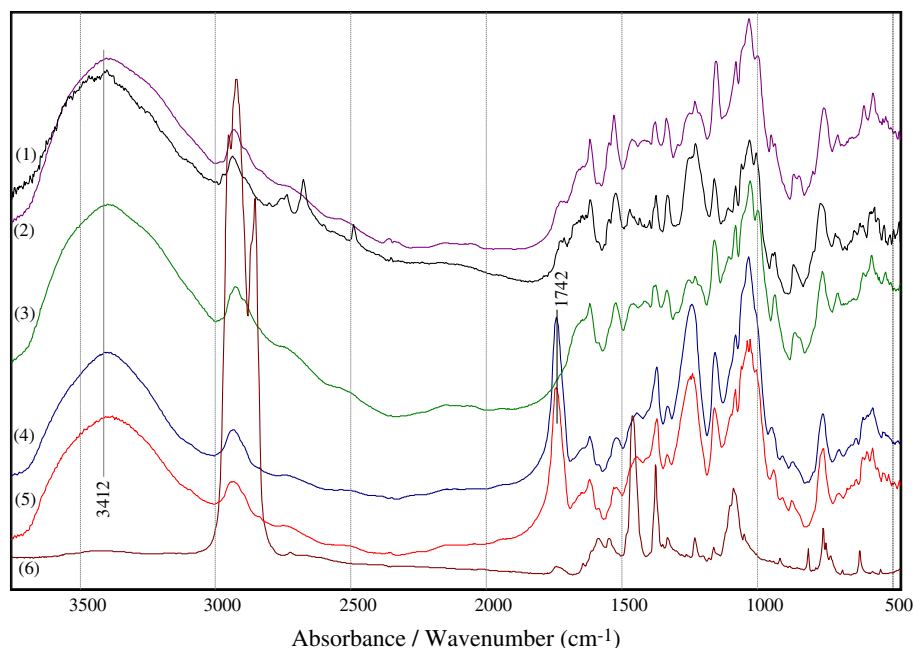
**Fig. 3** Theoretical IR-spectrum of dye, optimized at MP2/6-31++G\*\* level of approximation, and a scaling factor of 0.8929

peaks position of the pure dye (Fig. 4(6)) and in corresponding systems with CDs, additionally support the assumption about the adsorption of the dye on the CDs surfaces. The acetyl-fragments in the functionalized CDs are also affected weakly, due to the  $\nu_{\text{C=O}}$  stretching vibration in the Figs. 4(4) and (5) are influenced only with 2  $\text{cm}^{-1}$ , comparing with the data of the neutral CDs (see Fig. 2).

Thermal methods (mainly DSC, DTA and TGA) represent a very popular and wide spread analytical approach to the characterization of multicomponent systems such as inclusion compounds in the solid-state [39]. Such methods are commonly used for rapid preliminary qualitative investigations by comparison of the thermal stabilities of single components, their physical mixtures and the inclusion compound candidates. The thermal analyses of the samples under study show similar results for the mechanical mixtures of (**1**) with any of the CDs compared with their putative inclusion complexes. All the samples tend to lose weight



**Fig. 4** Solid-state IR-spectra of systems  $\alpha$ -CD/(**1**) (1),  $\beta$ -CD/(**1**) (2),  $\gamma$ -CD/(**1**) (3), Ac- $\beta$ -CD/(**1**) (4), Ac- $\gamma$ -CD/(**1**) (5) and the dye (**1**) (6), respectively



within the temperature range 315–350 °C, for example ((**1**)/CDs-(**I**)) 315–330 °C and ((**1**)/CDs-(**II**)) 340–350 °C, and at about 550 °C they lost 80% of their original weight. Differential Thermal Analyzer experiments were performed and they indicated that the systems display exothermic peaks within 320 °C ((**1**)/CDs-(**I**)) and 350 °C ((**1**)/CDs-(**II**)). These results provide further support of our assumption about the formation of supramolecular adsorption type of complexes. Surface morphologies of the supramolecular polymers are examined by SEM experiments (Scheme 2). The SEM images gave the macrostructure information about the Ac- $\beta$ -CD, Ac- $\gamma$ -CD as well as the corresponding “polymers”. Pure CDs and its functionalized derivatives showed preferentially the 3D regular structures. However, the surfaces of the five systems in the presence of (**1**) are different (Scheme 3). Such difference in the surface morphologies indicated that the presence of the (**1**), changes the macrostructures or the self-assembly of the CDs [33]. Only in the case of the system (**1**)/Ac- $\beta$ -CD the morphology of the plates that are observed differs from the rest of the samples. This could be explained with the fact that the starting material contains differently acetylated  $\beta$ -CD molecules, which are observed also in the corresponding system in the presence of the (**1**). In order to elucidate this phenomenon we performed the powder XRD experiment, thus proving the amorphous character of the CDs in the presence of (**1**).

## Conclusions

The interaction of native CDs, i.e.  $\alpha$ -,  $\beta$ - and  $\gamma$ -CD as well as the acetylated derivatives Ac- $\beta$ -CD and Ac- $\gamma$ -CD with

the organic asymmetric monomethylene cyanine dye, leads to the formation of “supramolecular polymers” when the molar ratio of the cyclodextrin towards organic dye is 1:1. The presence of the more than one acetylated form of the starting Ac- $\beta$ -CD as well as in corresponding supramolecular polymer plates leads to their different morphology. The physical properties and the correlation structure-spectroscopic data of the systems studied are elucidated by means of methods such as UV–VIS, IR-LD spectroscopy as well as  $^1\text{H-NMR}$ , SEM, powder XRD, and thermal methods both in solution and in the solid-state. Computational chemistry methods were employed with the purpose of elucidating the electronic structure and vibrational properties of the organic dye.

**Acknowledgments** The authors wish to thank Prof. T. Deligeorgiev for the guide-lines about the synthesis of the dye, as well as Prof. B. Ivanova for the quantum chemical calculations and helpful discussions. I.P. thanks the National Science Fund of Bulgarian Ministry of Education and Science, project DTK 02-25/2009.

## References

1. Szejtli, J., Osa, T. (eds.): *Comprehensive Supramolecular Chemistry*, vol. 3, Pergamon Press, Oxford (1996)
2. Saenger, W., Atwood, J.L., Davies, J.E.D., MacNicol, D.D. (eds): *Structural Aspects of Cyclodextrins and their Inclusion Complexes*. In *Inclusion Compounds*, vol. 2, pp. 231–259. Academic Press, New York (1984)
3. Bender, M., Komiyama, K.: *Cyclodextrin Chemistry*, chapter 3. Springer-Verlag, New York (1978)
4. Szejtli, J.: Introduction and general overview of cyclodextrin chemistry. *Chem. Rev.* **98**, 1743–1754 (1998)
5. Rekharsky, M., Inoue, Y.: Complexation thermodynamics of cyclodextrins. *Chem. Rev.* **98**, 1875–1918 (1998)

6. Connors, K.A.: The stability of cyclodextrin complexes in solution. *Chem. Rev.* **97**, 1325–1358 (1997)
7. Hapiot, F., Tilloy, S., Monflier, E.: Cyclodextrins as supramolecular hosts for organometallic complexes. *Chem. Rev.* **106**, 767–782 (2006)
8. Dodziuk, H. (ed.): *Cyclodextrins and Their Complexes*. Chemistry, Analytical Methods, Applications. Wiley-VCH Verlag GmbH&Co. KGaA, Weinheim (2006)
9. Wenz, G., Han, B., Muller, A.: Cyclodextrin rotaxanes and polyrotaxanes. *Chem. Rev.* **106**, 782–817 (2006)
10. Harada, A., Li, J., Kamachi, M.: Synthesis of a tubular polymer from threaded cyclodextrins. *Nature* **364**, 516–518 (1993)
11. Li, G., McGown, L.: Molecular nanotube aggregates of  $\beta$ - and  $\gamma$ -cyclodextrins linked by diphenylhexatrienes. *Science* **264**, 249–251 (1994)
12. Kaliappan, R., Maddipatla, M.M., Kaanumalle, L., Ramamurthy, V.: Crystal engineering principles applied to solution photochemistry: controlling the photodimerization of stilbazolium salts within  $\gamma$ -cyclodextrin and cucurbit[8]uril in water. *Photochem. Photobiol. Sci.* **6**, 737–741 (2007)
13. Ivanova, B., Simeonov, V., Arnaudov, M., Tsalev, D.: Linear-dichroic infrared spectroscopy-validation and experimental design of the new orientation technique of solid samples as suspension in nematic liquid crystal. *Spectrochim. Acta A* **67**, 66–75 (2007)
14. Ivanova, B., Spiteller, M.: Organic mandelates as promising materials with non-linear optical application. *Struct. Chem.* (2010). doi:10.1007/s11224-010-9635-5
15. Ivanova, B., Spiteller, M.: On the conformations and properties of the L-tryptophyl-containing peptides in solution, depending of the pH—theoretical study vs. experiments. *Biopolymers* **93**, 727–734 (2010)
16. Ivanova, B., Spiteller, M.: Noncentrosymmetric crystals with marked nonlinear optical properties. *J. Phys. Chem. A* **114**, 5099–5103 (2010)
17. Ivanova, B., Spiteller, M.: On the application of the organic barbiturates as NLO materials. *Cryst. Growth Des.* **10**, 2470–2474 (2010)
18. Frisch, M.J., Trucks, G.W., Schlegel, H.B., Scuseria, G.E., Robb, M.A., Cheeseman, J.R., Zakrzewski, V.G., Montgomery Jr, J.A., Stratmann, R.E., Burant, J.C., Dapprich, S., Millam, J.M., Daniels, A.D., Kudin, K.N., Strain, M.C., Farkas, Ö., Tomasi, J., Barone, V., Cossi, M., Cammi, R., Mennucci, B., Pomelli, C., Adamo, C., Clifford, S., Ochterski, J., Petersson, G.A., Ayala, P.Y., Cui, Q., Morokuma, K., Salvador, P., Dannenberg, J.J., Malick, D.K., Rabuck, A.D., Raghavachari, K., Foresman, J.B., Cioslowski, J., Ortiz, J.V., Baboul, A.G., Stefanov, B.B., Liu, G., Liashenko, A., Piskorz, P., Komáromi, I., Gomperts, R., Martin, R.L., Fox, D.J., Keith, T., Al-Laham, M.A., Peng, C.Y., Nanayakkara, A., Challacombe, M., Gill, P.M.W., Johnson, B., Chen, W., Wong, M., Andres, L., Gonzalez, C., Head-Gordon, M., Replogle, E.S., Pople, J.A.: *Gaussian 98*. Gaussian, Inc., Pittsburgh (1998)
19. “DALTON”, a molecular electronic structure program, Release 2.0. <http://www.kjemi.uio.no/software/dalton/dalton.html> (2005)
20. Zhurko, G.A., Zhurko, D.A.: ChemCraft: Tool for treatment of chemical data, Version build 08 (2005)
21. Deligeorgiev, T., Zaneva, D., Katerinopoulos, H., Kolev, V.: A novel method for the preparation of monomethine cyanine dyes. *Dyes Pigments* **41**, 49–54 (1999)
22. Benesi, H.A., Hildebrand, J.H.: A spectrophotometric investigation of the interaction of iodine with aromatic hydrocarbons. *J. Am. Chem. Soc.* **71**, 2703–2707 (1949)
23. Petinova, A., Metsov, S., Petkov, I., Stoyanov, S.: Photophysical behaviours of some 2-styrylindolium dyes in aqueous solutions and in the presence of cyclodextrins. *J. Incl. Phenom. Macrocycl. Chem.* **59**, 183–190 (2007)
24. Inigo, X., Garcia-Zubiri, G., Gonzalez-Gaitano, G., Sanchez, M., Ramon-Isasi, J.: FTIR study of dibenzofuran-2-carboxylic acid and its complexes with  $\beta$ -cyclodextrin. *Vib. Spectrosc.* **33**, 205–213 (2003)
25. Gaviraa, J.M., Hernanza, A., Bratu, I.: Dehydration of  $\beta$ -cyclodextrin: an IR  $\nu(\text{OH})$  band profile analysis. *Vib. Spectrosc.* **32**, 137–146 (2003)
26. de Sousa, F.B., Oliveira, M.F., Lula, I.S., Sansiviero, M., Cortes, M., Sinisterra, R.: Study of inclusion compound in solution involving tetracycline and  $\beta$ -cyclodextrin by FTIR-ATR. *Vib. Spectrosc.* **46**, 57–62 (2008)
27. Cannava, C., Crupi, V., Ficarra, P., Guardo, M., Majolino, D., Stancanelli, R., Venuti, V.: Physicochemical characterization of coumestrol/ $\beta$ -cyclodextrins inclusion complexes by UV-vis and FTIR-ATR spectroscopies. *Vib. Spectrosc.* **48**, 172–178 ((2008))
28. Roy, D., Deb, N., Ghosh, B., Mukherjee, A.: Inclusion of riboflavin in beta-cyclodextrin: a fluorimetric and absorption spectrometric study. *Spectrochim. Acta A* **73**, 201–204 (2009)
29. Hao, X., Li, N., Luo, H.: Determination of dextran sulfate sodium with crystal violet by triple-wavelength overlapping resonance Rayleigh scattering. *Spectrochim. Acta A* **71**, 1673–1677 (2009)
30. Zhang, M., Li, J., Zhanga, L., Chao, J.: Preparation and spectral investigation of inclusion complex of caffeic acid with hydroxypropyl- $\beta$ -cyclodextrin. *Spectrochim. Acta A* **71**, 1891–1895 (2009)
31. Harata, K.: Structural aspects of stereodifferentiation in the solid state. *Chem. Rev.* **98**, 1803–1828 (1998)
32. Lindner, K., Saenger, W.: Crystal and molecular structure of cyclohepta-amylose dodecahydrate. *Carbohydr. Res.* **99**, 103–115 (1982)
33. Saenger, W., Jacob, J., Gessler, K., Steiner, T., Hoffman, D., Sanbe, H., Koizumi, K., Smoth, S., Kakaha, T.: Structures of the common cyclodextrins and their larger analogues-beyond the doughnut. *Chem. Rev.* **98**, 1787–1802 (1998)
34. Kolev, T., Koleva, B.B., Seidel, R.W., Spiteller, M., Sheldrick, W.S.: New aspects on the origin of color in the solid state. Coherently shifting of the protons in violurate crystals. *Cryst. Growth Des.* **9**, 3348–3352 (2009)
35. Kolev, T., Tsanev, T., Kotov, S., Mayer-Figge, H., Spiteller, M., Sheldrick, W.S., Koleva, B.: Anyles of 4-benzoylpyridine-crystal structure and spectroscopic properties. *Dyes Pigments* **82**, 95–101 (2009)
36. Koleva, B.B., Kolev, T., Seidel, R., Spiteller, M., Mayer-Figge, H., Sheldrick, W.: Self-assembly of hydrogensquarates: crystal structures and properties. *J. Phys. Chem. A* **113**, 3088–3095 (2009)
37. Koleva, B.B., Kolev, T., Seidel, R.W., Mayer-Figge, H., Spiteller, M., Sheldrick, W.S.: On the origin of the color in the solid state. Crystal structure and optical and magnetic properties of 4-cyanopyridinium hydrogensquarate monohydrate. *J. Phys. Chem. A* **112**, 2899–2905 (2008)
38. Ivanova, B., Nikolova, R., Lamshöft, M., Tsanova, P., Petkov, I., Ivanov, P., Spiteller, M.: Surface interaction and self-assembly of cyclodextrins with organic dyes. *J. Incl. Phenom. Macrocycl. Chem.* **67**, 317–324 (2010)
39. Giordano, F., Novak, C., Moyano, J.: Thermal analysis of cyclodextrins and their inclusion compounds. *Thermochim. Acta* **380**, 123–151 (2001)